Journal of Magnetism and Magnetic Materials 465 (2018) 339–347

Contents lists available at ScienceDirect

Journal of Magnetism and Magnetic Materials

journal homepage: www.elsevier.com/locate/jmmm

Research articles

Influence of Al-doping on the structural, magnetic, and electrical properties of $La_{0.8}Ba_{0.2}Mn_{1-x}Al_xO_3$ $(0 \leqslant x \leqslant 0.25)$ manganites

J. Ardashti Saleh, I. Abdolhosseini Sarsari*, P. Kameli, H. Salamati

Department of Physics, Isfahan University of Technology, Isfahan 84156-83111, Iran

ARTICLE INFO

Keywords:
Manganite
Al doping
Sol-gel reaction
Doping
Ac susceptibility

ABSTRACT

We have studied the effect of Al doping on structural, magnetic and electrical properties of $La_{0.8}Ba_{0.2}Mn_{1-x}Al_xO_3$ $(0 \leqslant x \leqslant 0.25)$ manganite annealed in 750° and 1350° temperatures. Results show T_c decreases as Al ion substitution in Mn site. The magnetic susceptibility measurement shows Griffiths and spin-glass phase in aluminum-doped samples. Recently, Narreto et al., reported dynamic distortion and polaronic effects in the paramagnetic state of $La_{0.8}Ba_{0.2}Mn_{1-x}Al_xO_3$ manganites. Here we completed the phase diagram and show an occurrence of the spin-glass state in this manganite. The resistivity measurement shows, T_{MIT} (metal-insulator) transition temperatures decreases and the system become an insulator. The insulator–metal transition occurs for the undoped sample annealed at the low temperature in near 165 K, while this transition is weak for the undoped sample annealed at high temperature due to oxygen non-stoichiometry. Using three models VIZ., Adiabatic small polaron hoping, Variable range hopping, and Percolation model, the resistivity have been studied.

1. Introduction

During the last two decades, perovskite manganites are widely studied, after the discovery of their interesting physical properties. Perovskite manganites with the formula $A_{1-x}B_xMnO_3$ (A is trivalent rare-earth cation such as La, Sm, Nd, Pr, …, and B is divalent alkali or alkaline earth cation such as Sr, Ca, Ba or other vacancies) is any of a variety of manganese oxides with strongly correlated electrons [1–4]. Doping in A and B sites provides cation size mismatch on ABO_3 perovskite structures, measured by the tolerance factor, that impact on the structures of samples. Undoped $LaMnO_3$, as a typical compound, is an antiferromagnetic (AFM) insulator. However, when some parts of La site are substituted by a divalent metal ion (like Ca, Ba or Sr), the compound becomes metallic ferromagnetic (FM) and introduce a ferromagnetic–paramagnetic (PM) transition. The fundamental feature of the magnetic properties and conduction mechanism in manganites can be explained qualitatively, by the double exchange (DE) mechanism, Jahn–Teller distortion and electron–phonon interactions in manganites. The DE mechanism is responsible for the ferromagnetic state due to the transfer of the itinerant e_g electron between the Mn^{3+}–O–Mn^{4+} bond through the O^{2-} ion due to on-site Hund's coupling

[5–7]. Jahn–Teller distortion breaks the degeneracy of the e_g orbitals. There is the close conenection between the Jahn–Teller distortions and the polarons and this coupling is locally present in the metallic and insulating phases [8].

To understand the structural, magnetic and transport properties of $La_{1-x}A_xMnO_3$ manganites, several studies have been reported the A-site doping with divalent ions [9–13]. A substitution at Mn (B-site) dramatically affects the structural, magnetic and transport properties of these compounds. As trivalent La^{3+} ions are replaced with a divalent Ba^{2+} in $LaMnO_3$ manganite, some of the manganese ion valence changed from Mn^{3+} (with the electronic configuration $3d^4$, $t_{2g}^3\ e_g^1$, S = 2) to Mn^{4+} (with the electronic configuration $3d^3$, $t_{2g}^3\ e_g^0$, S = 3/2) due to inserting holes into the this material. These holes permit charge transfer in the e_g state which is highly hybridized with the oxygen 2p state. In the following, replacing the Mn^{3+} ion with trivalent Al changes the relative fraction of Mn^{3+} ions, in other words, the ratio of Mn^{3+} to Mn^{4+} [14]. This replacement can cause a large changes in corresponding manganite. Al^{3+} does not possess a magnetic moment and does not participate in the magnetic interactions. Also, the Al ion has a smaller size (0.535 Å) than that a Mn ion (0.645 Å) and makes an increase in the structural stress [15,14]. Based on the foregoing, the $La_{1-x}Ba_xMn_{1-x}Al_xO_3$ manganite is one of the most attractive manganites. The $La_{1-x}Ba_xMn_{1-x}Al_xO_3$ manganite having the T_C and T_N (Neel temperature) in the temperature range of 295–50 K for doping range of $0 \leqslant x \leqslant 0.8$ [15].

Various models used to explain the conductive mechanism in perovskite manganites. Among these models, we point out the Variable Range Hopping (VRH), the Adiabatic Small Polaron Hoping (ASPH), percolation and Zhang models [16,17]. The ASPH model proposed for

* Corresponding author.
E-mail address: abdolhosseini@cc.iut.ac.ir (I.A. Sarsari).

https://doi.org/10.1016/j.jmmm.2018.06.014
Received 6 February 2018; Received in revised form 7 May 2018; Accepted 8 June 2018

high temperature $\left(T > \frac{\theta_D}{2}\right)$ resistivity in the paramagnetic regime at temperatures higher than T_C. According to this model, the activation energy E_0 is the depth of the local potential barrier of a trapped polaron [18].

The VRH model proposed to explain conduction mechanism for manganites via thermally activated small polarons in the adiabatic regime ($T < \frac{\theta_D}{2}$). In the VRH model, the carriers are localized by random potential fluctuation. In percolation model, there is competition between FM and PM phases [16], while according to Zhang model [17], a perovskite grain can be divided into the core and shell phases in which the core phases have higher Curie temperature and magnetization [17].

In this work, the B-site (Mn-site) of the $La_{0.80}Ba_{0.20}Mn_{1-x}Al_xO_3$ ($0 \leqslant x \leqslant 0.25$) compound was gradually substituted by the Al^{3+} ion. Using XRD, ac magnetic susceptibility, and electrical resistivity measurements, the changes in the structural, magnetic, and electrical properties of the $La^{3+}_{0.80}Ba^{2+}_{0.20}Mn^{3+}_{0.8-x}Mn^{4+}_{0.2}Al^{3+}_xO^{2}_3$ (x = 0, 0.10, 0.15, 0.20, and 0.25) manganite polycrystalline samples have been reported.

In this paper, we have tried to extend our knowledge about spin glass phase and Griffith's phase based on the partial substitution of Mn site by Al, with a significant novel result. In this project samples prepared via the sol–gel method and annealed at 2 different temperature to investigate size effect, too.

2. Experiment details

The $La_{0.8}Ba_{0.2}Mn_{1-x}Al_xO_3$ samples (x = 0, 0.10, 0.15, 0.20, and 0.25) have been successfully prepared using sol–gel method. The starting material with the purity of 99.9% are used as follows:

$Ba(NO_3)_2$ (Barium nitrate), $La(NO_3)_3$.$6H_2O$ (Lanthanum nitrate), $Mn(NO_3)_2$.$4H_2O$ (Manganese nitrate), $Al(NO_3)_3$.$9H_2O$ (Aluminum nitrate), $C_6H_8O_7$(Citric acid), and $C_{10}H_{16}N_2O_8$(Ethylene diamine tetra-acetic acid or EDTA).

PH adjusting to 7, the nitrates was dissolved in deionized water and mixed with EDTA. The chemical equation for x = 0, 0.10, 0.15, 0.20, and 0.25 samples in $La_{0.8}Ba_{0.2}Mn_{1-x}Al_xO_3$ is as following:

$$[\alpha\ La(NO_3)_3.\ 6\ H_2O_{(aq)} + \beta\ Ba(NO_3)_{2(aq)} + \gamma\ Mn(NO_3)_2.\ 4H_2O_{(aq)} + \sigma\ Al(NO_3)_3.\ 9H_2O_{(aq)}] + 3[\eta\ C_6H_8O_7.\ H_2O_{(aq)}] + 2[C_{10}H_{16}N_2O_{8(aq)}] \rightarrow \phi La_{0.80}Ba_{0.20}Mn_{1-x}Al_xO_{3(s)} + \omega\ CO_{2(g)} + \mu H_2O_{(g)} + \theta N_{2(g)}$$

where the Greek letters represent the amount of each compound. The molar ratio of acid, EDTA and nitrate materials were taken 1:2:3. The solution changed to a gel when it exposed to heat for drying, (the temperature increased to 220° with rate of $\frac{1^{0}C}{6min}$). The dry powders was subjected to high energy ball milling for 2 h in stainless steel vial and balls at rotational speed of 400 rpm using planetary ball milling machine. 2 h Milling and 5 h sintering at 450°C result in homogenous composition.

Annealing in air at two different temperatures, 750 °C for 5 h and 1350 °C for 48 h, samples make a different grain size and grain boundaries (GBs) in these compounds [19–21]. LBMO phases are beginning to grow at temperatures higher than 600°C [22]. The slab samples were pressed under 354Psi (31.9 MPa) pressure with typical dimensions of about 1.30 × 3.22 × 3.15 mm^3.

GBs growth, with increasing temperature from 750 °C to 1350 °C, change their magnetic and electrical properties. We labeled samples with doping level of x = 0, 0.10, 0.15, 0.20, and 0.25 that annealed in 750°C as: L0, L10, L15, L20, and L25 (L refers to low temperature), while those annealed in 1350°C labeled as: H0, H10, H15, H20, and H25 (H refers to high temperature), respectively.

Ultimately, we studied the structural, magnetic and electrical effects of Al doping on Mn sites in $La_{0.8}Ba_{0.2}Mn_{1-x}Al_xO_3$, by using XRD, SEM, ac susceptibility analysis and measuring the electrical resistivity for two types of the composition prepared at different temperatures. Phase formation and crystal structure of samples were studied by XRD pattern using Cu-$k\alpha$ radiation source with wavelength of $\lambda = 1.5406$ Å in the 2θ range from 20° to 80°, with a step size of 0.05°.

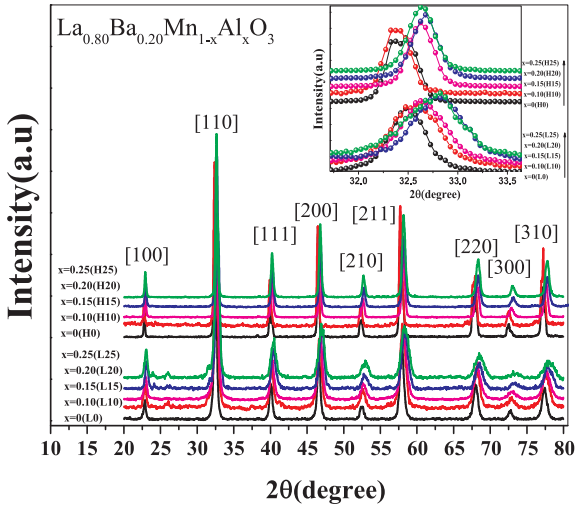

Fig. 1. The XRD pattern of all samples at room temperature that were sintered at in 750 °C and 1350 °C. Inset shows zoomed [1 1 0] peak. A slightly shift to right hand side can be seen in all peaks with increasing Al ion substitution.

To study the magnetic properties of the samples, the ac susceptibility measurements were performed using a Lake Shore Ac Susceptometer (Model 7000) in 333 Hz frequency and 800 A/m field. Also, we used conventional four probe method for measuring the electrical resistivity, using a Leybold closed cycle refrigerator.

3. Results and discussion

Fig. 1 shows the room temperature X-ray diffraction (XRD) patterns of $La_{0.8}Ba_{0.2}Mn_{1-x}Al_xO_3$ (x = 0–0.25) samples sintered at 1350°C and 750°C. The XRD pattern Rietveld refinement of all samples, using the FULLPROF software and Pseudo-Voigt function shows single phase with $R\bar{3}c$ space group for H series of samples (for instance H0 sample's Rietveld analysis was shown in Fig. 2). For L series of samples we also used $R\bar{3}c$ space group for refinement. The additional peaks around 25 degrees in XRD patterns of Al-doped samples calcinated at low temperature belong to aluminum oxyhydroxides. We suppose that as portion of grain boundaries but since its relative phase fraction is low, it

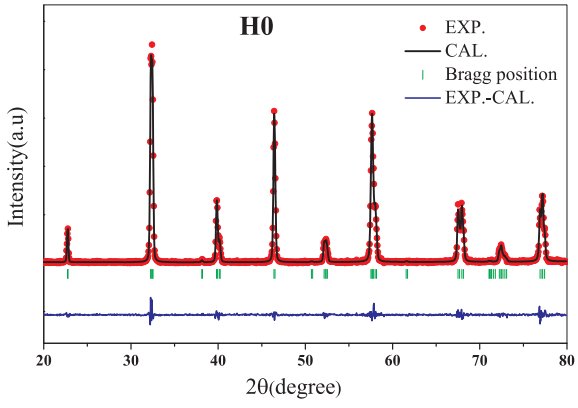

Fig. 2. The observed and calculated XRD patterns of H0 sample by Reitveld analysis. Red points (circle) shows the results of through experiments, black lines obtained from calculation, the blue line shows the difference between calculation and the results of experiment and eventually green vertical lines, points out the Bragg positions. (For interpretation of the references to colour in this figure legend, the reader is referred to the web version of this article.)